

Asbestos: When the Dust Settles—An Imaging Review of Asbestos-related Disease¹

Huw D. Roach, FRCR • Gareth J. Davies, FRCR • Richard Attanoos, MRCPath • Michael Crane, FRCR • Haydn Adams, FRCR • Siân Phillips, FRCR

Asbestos-related neoplastic and nonneoplastic diseases of the lungs and pleura range from pleural effusion and pleural plaques to lung cancer and malignant mesothelioma. Pleural effusions are typically hemorrhagic exudates of mixed cellularity but do not typically contain asbestos bodies. The classic distribution of pleural plaques seen on chest radiographs is the posterolateral chest wall between the seventh and tenth ribs, lateral chest wall between the sixth and ninth ribs, the dome of the diaphragm, and the mediastinal pleura. Computed tomographic (CT) findings support this distribution but also show anterior and paravertebral plaques not well shown at chest radiography. Imaging features of diffuse pleural thickening include a continuous sheet, often involving the costophrenic angles and apices, that rarely calcifies. The typical CT features of round atelectasis are of a round or oval mass that abuts the pleura, a “comet tail” of bronchovascular structures going into the mass, and thickening of the adjacent pleura. Features of asbestosis on chest radiographs include ground-glass opacification, small nodular opacities, “shaggy” cardiac silhouette, and ill-defined diaphragmatic contours. CT, however, is more sensitive in their detection. Chest radiography in patients with malignant mesothelioma may show an effusion, pleural thickening, and as the tumor progresses, a more lobulated outline. CT can help identify the disease in its early stages. Asbestos-related cancers can occur anywhere in the lungs. Recognition of the clinical, radiologic, and pathologic features of these diseases will be important for some years to come.

©RSNA, 2002

Abbreviation: ILO = International Labour Organization

Index terms: Asbestos • Asbestosis, 60.773, 60.774 • Lung neoplasms, 60.774, 66.3254 • Mesothelioma, 66.3254 • Peritoneum, diseases, 60.773, 60.774, 66.3254 • Pleura, diseases, 60.773, 66.3254

RadioGraphics 2002; 22:S167–S184

¹From the Department of Radiology, University Hospital of Wales, Heath Park, Cardiff CF14 4XW, United Kingdom (H.D.R., G.J.D.); Departments of Histopathology (R.A.) and Radiology (M.C., H.A.), Llandough Hospital, Cardiff, United Kingdom; and Department of Radiology, Princess of Wales Hospital, Bridgend, United Kingdom (S.P.). Presented as an education exhibit at the 2001 RSNA scientific assembly. Received February 1, 2002; revision requested March 7 and received June 3; accepted June 19. **Address correspondence to** H.D.R. (e-mail: huwroach@doctors.org.uk).

©RSNA, 2002

Introduction

The commonly encountered asbestos-induced diseases mainly relate to the thorax. The main asbestos-related conditions and diseases include pleural effusion, pleural plaques, diffuse pleural thickening, asbestosis, malignant mesothelioma, and bronchogenic carcinoma. In this article, we discuss asbestos and asbestos exposure, briefly describe the International Labour Organization (ILO) Classification of radiographs of pneumoconioses, and review the typical imaging characteristics of asbestos-related diseases, with emphasis on histopathologic correlation.

Asbestos and Asbestos Exposure

Asbestos is the name given to a group of naturally occurring silicate minerals whose fire-resistant properties have been known for thousands of years. Asbestos deposits are widely distributed throughout the world, with most being found in mountain-forming regions. Techniques for spinning and weaving the fibers were developed in the 19th century and led to a rapid increase in their use.

Asbestos is not combustible, has great tensile strength, and has good frictional properties. It is a good thermal and electrical insulator, and is durable, strong, and flexible. These properties have led to its use in many commercial and domestic settings, including insulation materials, brake pads and linings, household products, floor tiles, electric wiring, paints, and cements.

The fibers of asbestos can be broadly classified into two main groups, namely serpentine fibers, which are curly and flexible, and amphibole fibers, which are stiff and straight. Chrysotile (white asbestos) is the most important serpentine fiber. Crocidolite (blue asbestos) and amosite (brown asbestos) are the most notable amphibole fibers. The other commercially used asbestos types are anthophyllite (a common contaminant of industrial talc), tremolite (a common contaminant of chrysotile), and actinolite.

Chrysotile is essentially the only type of asbestos significantly used today. The current products are mainly cements, with friction materials and plastics making up the rest. Most of the major natural asbestos deposits are chrysotile, with crocidolite and amosite deposits being found in parts of southern Africa. This distribution of fiber types may have relevance regarding the geographic distribution and prevalence of asbestos-related diseases.

The biohazard of asbestos arises from inhalation of the fibers. Physical properties, such as length, diameter, length-to-width (aspect) ratio, and texture, and chemical properties are believed to be determinants of fiber distribution and disease severity. The amphiboles (eg, amosite and crocidolite) are widely accepted as being more hazardous than chrysotile. They are dusty and biopersistent owing to their structure and straight, needlelike fibers. Chrysotile has a softer texture and curly fibers, giving it a relatively broad cross-sectional area. Fewer fibers are therefore inhaled, and the body eliminates them more easily via the mucociliary elevator or lymphatic vessels. Chrysotile also fragments and is more soluble (1).

Of those fibers that remain in the lung, some (mainly amphiboles) become coated with ferritin to form asbestos (or ferruginous) bodies.

Exposure to asbestos arises from mining and processing of asbestos and manufacture of asbestos products. The dangers of asbestos inhalation have been known since the early 20th century. Beginning in the 1970s, countries gradually prohibited the use of amphiboles and sprayed-on friable insulation materials (routinely used in Europe and the United States after World War II) in favor of the chrysotile products used today. Prevalence of asbestos-related diseases is still increasing, however, owing to the long latency between exposure and onset of disease. Even after the change in asbestos policy in the 1970s, it is forecast that the prevalence of asbestos-related diseases such as malignant mesothelioma will not decrease for another 10–20 years in the United Kingdom (2). This decline may occur even later in parts of Eastern Europe and Asia, where controls have been less stringent (3).

The sufferers of asbestos-related diseases and their dependents can be eligible for financial compensation. In the United Kingdom, sufferers of asbestosis; diffuse mesothelioma of pleura, pericardium, or peritoneum; diffuse pleural thickening; or carcinoma of the lung, accompanied by asbestosis or diffuse pleural thickening, contracted through work-related exposure are entitled to compensation and disablement benefit. When liable employers have ceased trading or there is little chance of obtaining compensation from them (eg, if there has been no demonstrable negligence or breach of procedure), acts of Parliament allow state-funded benefit and compensation payments.

There are defined plain radiographic criteria for the diagnosis of diffuse pleural thickening with

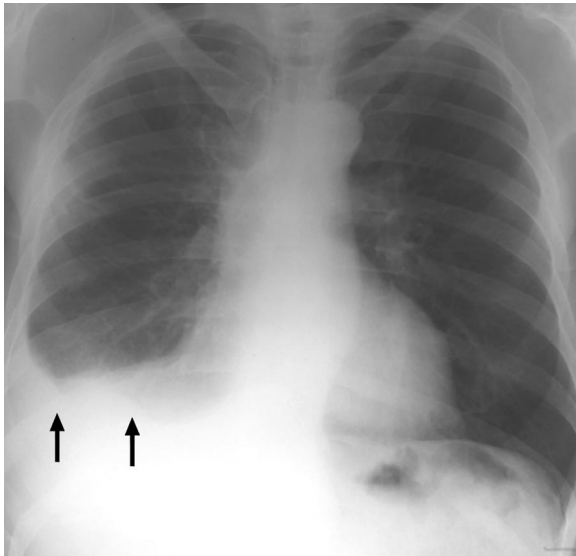


Figure 1. Posteroanterior radiograph of an asbestos-exposed patient shows a right-sided pleural effusion (arrows).

regard to eligibility for compensation (4). Computed tomographic (CT) evidence is not included at present in the United Kingdom. There are no corresponding officially defined radiologic criteria for the diagnosis of asbestosis, with assessment based on a combination of clinical and plain radiographic information.

The severity of disability and corresponding level of compensation for asbestos-related disease in the United Kingdom are decided by means of clinical judgment of the assessing panel rather than any strictly defined parameters. A patient can sue her or his employer or former employer for any asbestos-related disease irrespective of whether the criteria for state-funded compensation are met.

ILO Classification

The 1980 ILO Classification of radiographs of the pneumoconioses was designed to aid the systematic recording of radiographic changes caused by dust inhalation (5). It is intended to facilitate international epidemiologic comparisons through the coding of radiographic abnormalities in a simple reproducible manner by means of comparison with a standard set of radiographs. It describes the classification of findings on a posteroanterior chest radiograph but does not define pathologic entities. Neither does it consider occupation nor define a level of abnormality that would be considered worthy of compensation (6).

The classification includes written text and a set of notes, but comparison with the standard radiographs is important. These standard images

are designed to reduce interobserver variability (5,6).

As stated earlier, the system describes changes on a posteroanterior chest radiograph. If additional views (eg, oblique, lateral) are available, their contribution can be recorded as comments, but they cannot form part of the quantitative part of the grading. The technical quality of the radiograph is also graded.

The reporting system covers parenchymal and pleural abnormalities. The presence of small parenchymal abnormalities is defined according to shape, size, and profusion with the use of a letter and number system in reference to the standard radiographs. Large opacities are those greater than 1 cm in diameter. Their presence is recorded, and their size classified. Pleural thickening is classified according to its site (eg, chest wall, diaphragm, mediastinum), width, extent, and calcification. Pleural changes are recorded separately for the right and left lungs.

A series of symbols is also available to address other relevant features that might be present (eg, honeycombing, coalescence of opacities, and suspicion of malignancy).

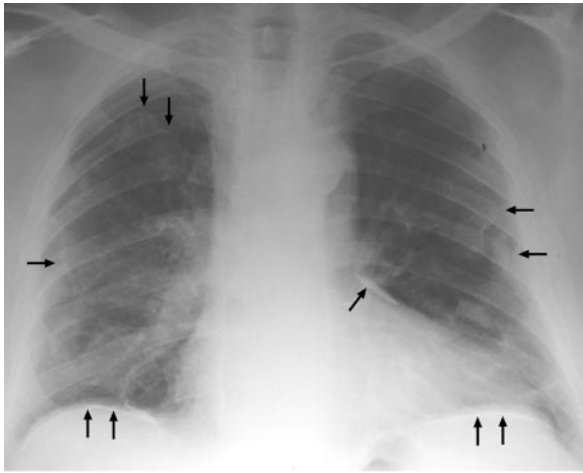
Although high-resolution CT is more sensitive than plain radiography in the detection of early asbestos-related pleural and parenchymal changes (7) and the correlation between high-resolution CT and pathologic findings has been established (7), we are not aware of an internationally accepted and widely used CT classification equivalent to the ILO Classification for plain radiographs. However, some have been proposed (7,8). One of the problems is that the findings at CT are nonspecific and separation of subnormal and occupationally induced changes may be difficult. At present, chest radiography is the main screening tool, with CT reserved for problem solving (eg, clarifying pleural thickening, staging mesothelioma, looking for lung cancer, and planning biopsy) (9).

Benign Pleural Disease

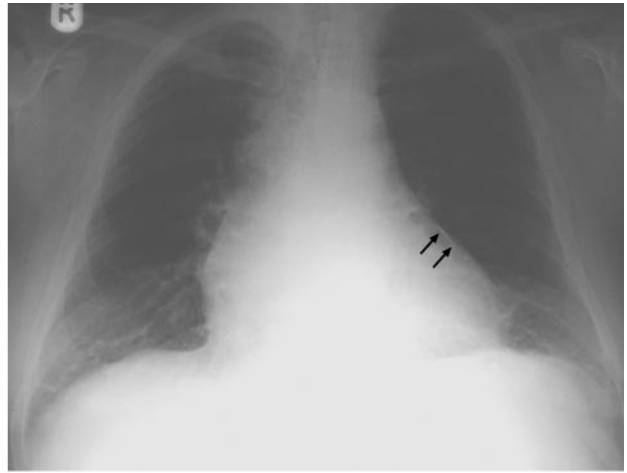
Pleural disease is the most commonly encountered manifestation of asbestos-related disease. The pleurae are thought to be more sensitive to asbestos than the lung parenchyma (1). Pleural disease can occur as pleural effusion, plaques, or thickening, as well as atelectasis.

Pleural Effusion

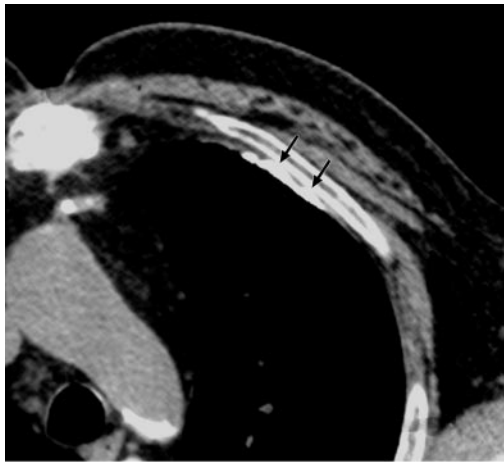
Benign pleural effusions are thought to be the earliest pleural-based phenomenon (1) (Fig 1). They were first described in relation to asbestos



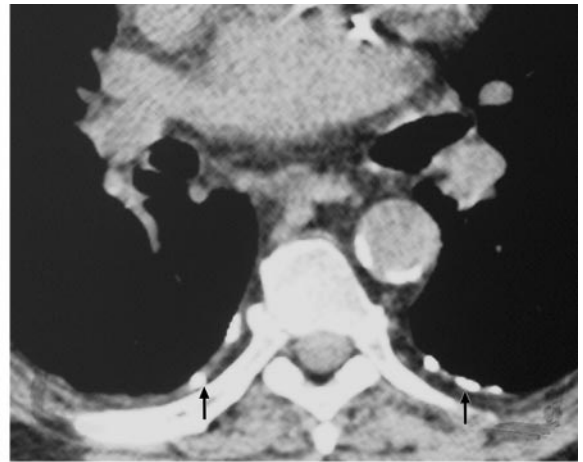
2.



3a.



3b.



3c.

Figures 2, 3. (2) Posteroanterior radiograph shows extensive calcified pleural plaques (arrows) that affect the chest wall, diaphragm, and pericardium. The costophrenic angles and apices are spared. (3a) Posteroanterior radiograph of an obese patient shows only a small amount of pericardial calcification (arrows). (3b, 3c) Axial CT scans obtained with soft-tissue window settings show calcified anterior and paravertebral plaques (arrows) not seen on the radiograph.

exposure in the 1960s (1,10). Their exact prevalence is unknown, as many are subclinical (1, 10,11). They usually occur within 10 years of exposure (12), but they can also develop much later. They are typically hemorrhagic exudates of mixed cellularity and usually do not contain asbestos bodies (11). The effusions usually resolve over a few months but can persist or recur (1). Diffuse pleural thickening is commonly seen after resolution. The development of effusions is thought to be exposure-dependent (11), but they can occur even after minimal exposure (13) and

can be dependent on occupation (11). Pleural effusions are a common entity, and their diagnosis is reliant largely on the exclusion of other causes of effusions in an asbestos-exposed patient. The differential diagnosis for an exudative effusion includes consideration of parapneumonic effusion, tuberculosis, malignancy, pulmonary embolus, pancreatitis, connective tissue disease, trauma, azotemia, and drugs.

Pleural Plaques

The most common manifestation of asbestos exposure is pleural plaques, which are discrete areas of fibrosis that usually arise from the parietal pleura but may arise from visceral pleura. They

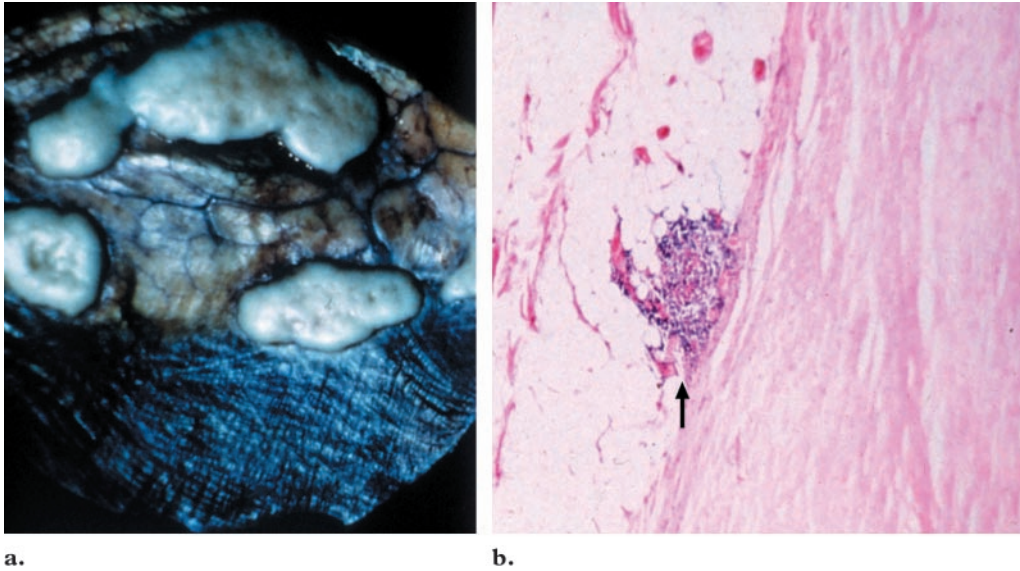


Figure 5. (a) Photograph (original magnification, approximately $\times 0.5$) shows multiple raised pearly plaques that arise from the parietal pleura. (b) Photomicrograph (original magnification, approximately $\times 250$; hematoxylin-eosin stain) shows paucicellular hyalinized pleural plaque with a basket-weave pattern and focal lymphocytic aggregate (arrow).



Figure 4. Axial high-resolution CT scan obtained with lung windows shows uncalcified anterior pleural plaque (arrows).

tend to occur 20–30 years after exposure (1). The classic distribution of plaques seen on chest radiographs is the posterolateral chest wall between the seventh and tenth ribs, lateral chest wall between the sixth and ninth ribs, the dome of the diaphragm (virtually pathognomonic), and the mediastinal pleura (1,14) (Fig 2). The apices and costophrenic angles are typically spared. CT findings support this distribution but also show anterior and paravertebral plaques that are not well

demonstrated at chest radiography (Fig 3). Some authors report a left-sided predominance (15), whereas others have found none (16).

The size and number of plaques are variable. Calcification is reported in 10%–15% of cases (1) (Fig 4). At histologic examination, the plaques are relatively acellular, with a “basket-weave” appearance of collagen bundles (Fig 5). Asbestos fibers (usually chrysotile) are often seen, but asbestos bodies are usually absent (1). The pathogenesis of plaques is uncertain, but it is thought that fibers reach the pleura via lymphatic channels and cause an inflammatory reaction. Other mechanisms could be hematogenous carriage or direct migration (1,17,18).

Although the ILO uses posteroanterior chest radiography to assess pleural disease, conventional and high-resolution CT are more sensitive (1). One study reports that conventional CT revealed plaques in 95% of the study population compared with 59% at chest radiography (19), whereas another claims high-resolution CT depicts 100% of plaques versus 93% with conventional CT (20). Friedman et al (21) showed that high-resolution CT had a 97% sensitivity and 100% specificity in the detection of pleural disease as a whole; they recommended it particularly for distinguishing pleural disease from extrapleural fat.

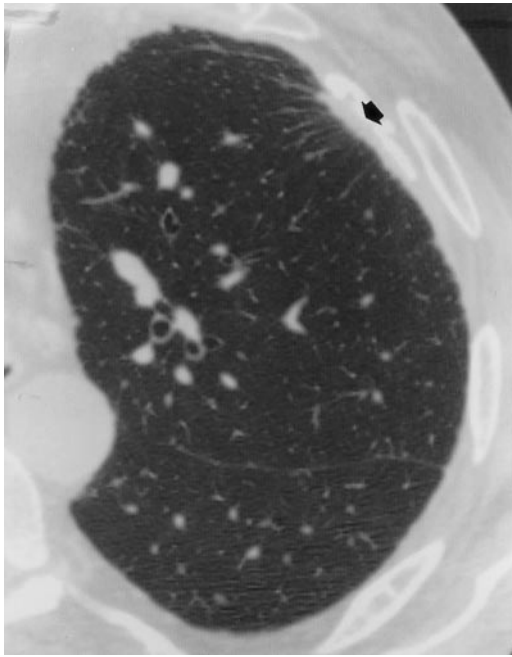


Figure 6. Axial high-resolution CT scan shows an anterior pleural plaque with associated linear opacities that project into the underlying lung.

Visceral pleural plaques are associated with abnormality in the adjacent lung parenchyma, including short interstitial lines that radiate from the plaque (so-called hairy plaques) or more extensive parenchymal opacities (Fig 6). The differential diagnosis for pleural plaques should include adipose tissue, rib fracture, companion shadows for ribs, and other pleural masses such as metastases.

Diffuse Pleural Thickening

Diffuse pleural thickening is less specific for asbestos exposure because other causes of exudative effusions can lead to it. It results from thickening and fibrosis of the visceral pleura, which leads to fusion with the parietal pleura (Fig 7), and is preceded by benign pleural effusion (1) (Fig 8). Histologically, there is similarity between pleural thickening and plaques, except that fusion of the pleural layers is suggestive of more intense inflammation (22). The underlying process is thought to be inflammation and fibrosis of lymphatic vessels and may be a direct extension of lung fibrosis (23).

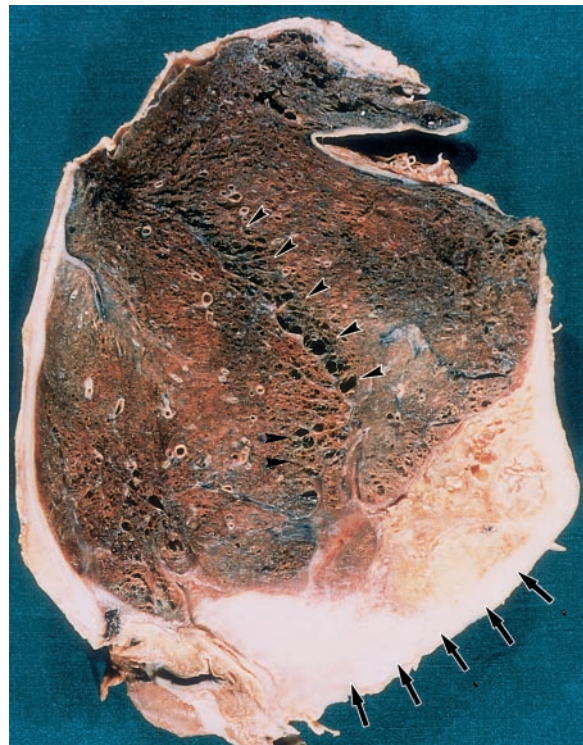


Figure 7. Photograph (original magnification, approximately $\times 0.5$) of a whole lung section shows circumferential diffuse pleural thickening (arrows). The lung parenchyma shows honeycombing that indicates asbestosis (arrowheads).

Imaging features include a continuous sheet, often involving the costophrenic angles and apices, that rarely calcifies (Fig 9).

There have been different definitions of diffuse pleural thickening derived from chest radiographic and CT criteria. With regard to state compensation or disability benefit in the United Kingdom, the plain radiographic criteria used for diffuse pleural thickening are the following: it may be unilateral or bilateral; it must cover at least 25% of the total chest wall on a chest radiograph (50% if unilateral); and it must extend to a thickness of at least 5 mm in at least one site on the chest radiograph (4). McLoud et al (24) defined diffuse pleural thickening on chest radiographs as a smooth uninterrupted pleural opacity that extends over at least one-quarter of the chest wall with or without obliteration of the costophrenic angle (1,24). Lynch et al (25) use CT criteria of a continuous sheet of pleural thickening more than 5 cm wide, more than 8 cm in craniocaudal extent, and more than 3 mm thick.

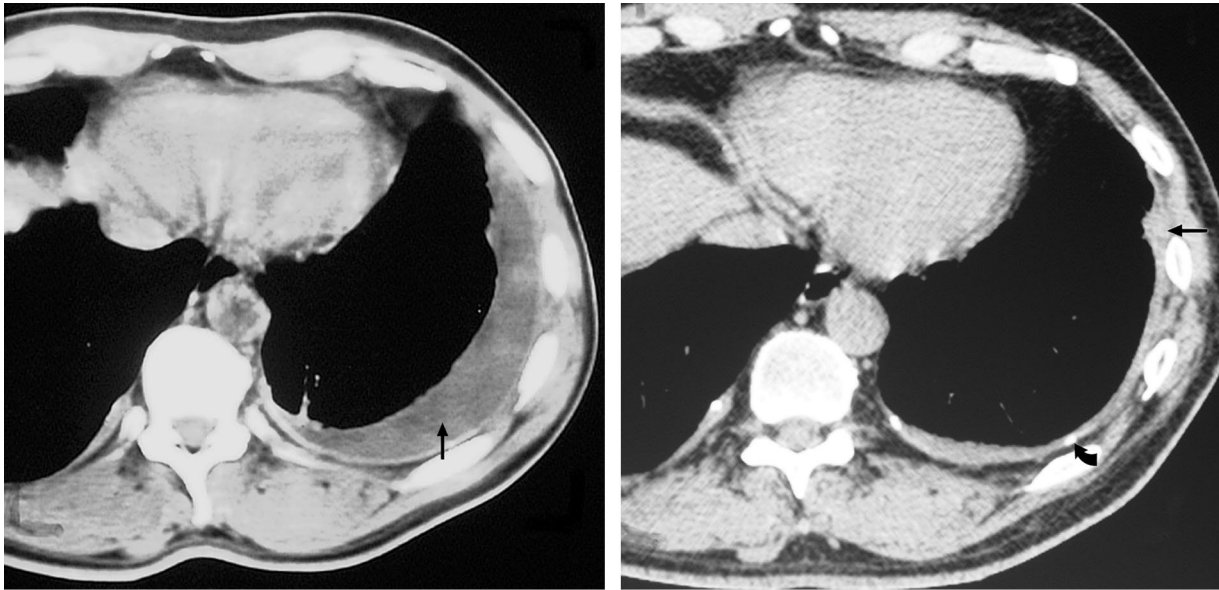


Figure 8. (a) Axial CT scan of an asbestos-exposed person shows a left-sided pleural effusion (arrow). (b) Axial CT scan obtained 2 years later shows circumferential pleural thickening that extends into the major fissure (straight arrow) and contains flecks of calcification (curved arrow).

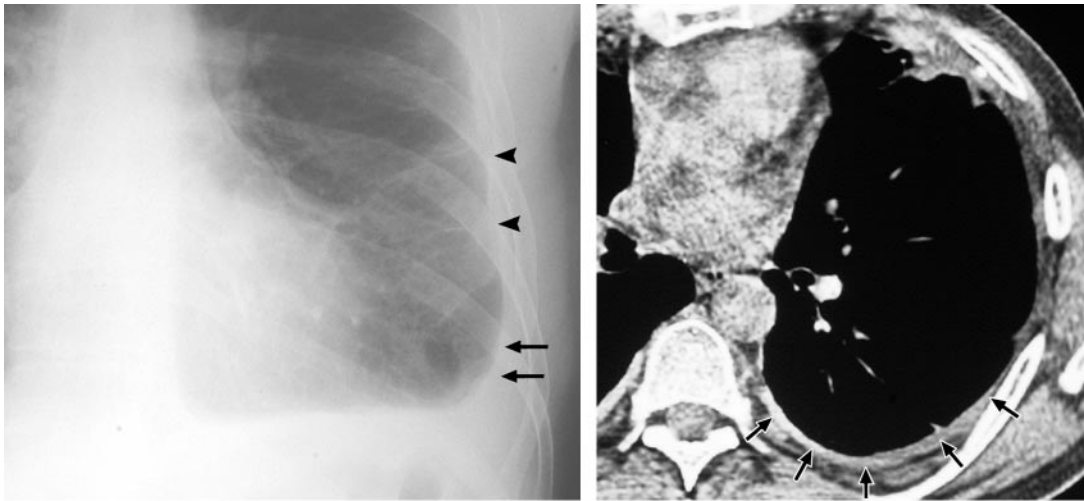


Figure 9. (a) Posteroanterior radiograph shows pleural thickening with obliteration of the left costophrenic angle (arrows). There are also some associated linear parenchymal opacities (arrowheads). (b) Axial CT scan of the same patient shows circumferential pleural thickening (arrows).

Differentiation of pleural thickening from plaques can be difficult. Apart from the appearances mentioned above, diffuse pleural thickening has ill-defined, irregular margins from all angles, whereas plaques are well defined and do not tend to extend for more than four interspaces unless

they are confluent. Diffuse pleural thickening involves the interlobar fissures (visceral pleura), whereas plaques normally do not (14,24,25). The differential diagnosis for diffuse pleural thickening includes organizing effusion, chronic infection

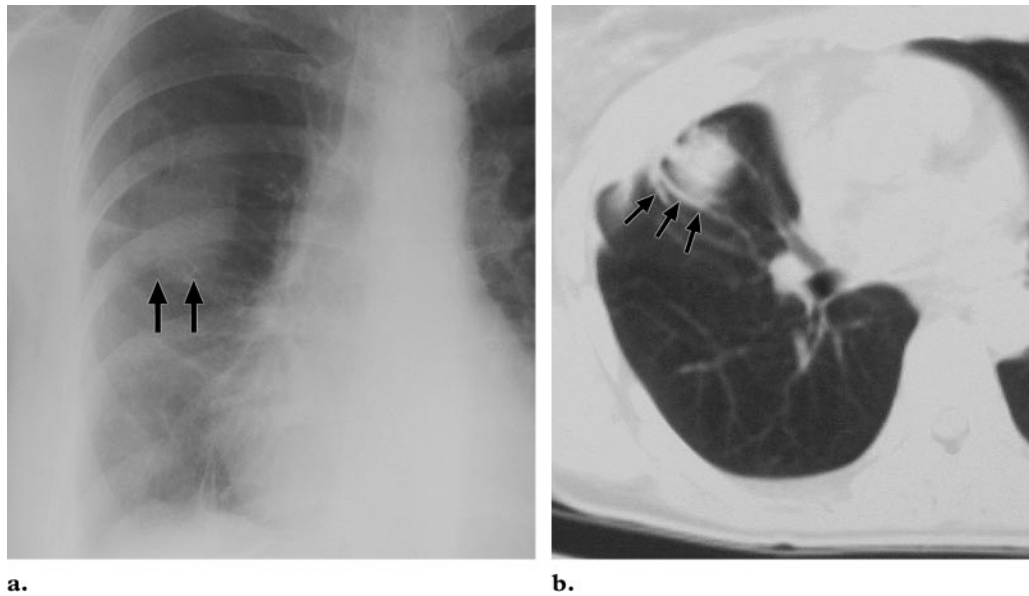


Figure 10. (a) Posteroanterior radiograph shows an opacity in the right middle zone (arrows). (b) Axial CT scan of the same patient shows a peripheral mass that abuts thickened pleura, with comet tail distortion of the vascular structures (arrows).

(eg, tuberculosis), connective tissue diseases, talcosis, pleural metastases, and mesothelioma.

CT is more sensitive and specific than chest radiography in the detection of diffuse pleural thickening. Al Jarad et al (19) found that CT depicted diffuse pleural thickening in all of the patients in their series, whereas chest radiography showed only 70%. The advantage of high-resolution CT over conventional CT is not clear-cut. Aberle et al (20) found that high-resolution CT could miss pleural thickening depicted with conventional CT owing to the gaps between sections. Friedman et al (21) quoted 97% sensitivity and 100% specificity for pleural disease as a whole, but Aberle et al (26) showed that in their series only three of seven patients with pleural thickening were detected with high-resolution CT compared with all seven with conventional CT.

Some authors have found reasonable correlation between CT appearances of diffuse pleural thickening and respiratory impairment (27), a finding that contrasts with plaques, which are usually asymptomatic.

Round Atelectasis

The pathogenesis of round atelectasis is not certain, but it is thought to be due to an inflammatory reaction and fibrosis in the superficial layer of the pleura. As the fibrous tissue matures, it contracts, causing pleura to fold into the lung, which in turn causes atelectasis (28). Asbestos-related

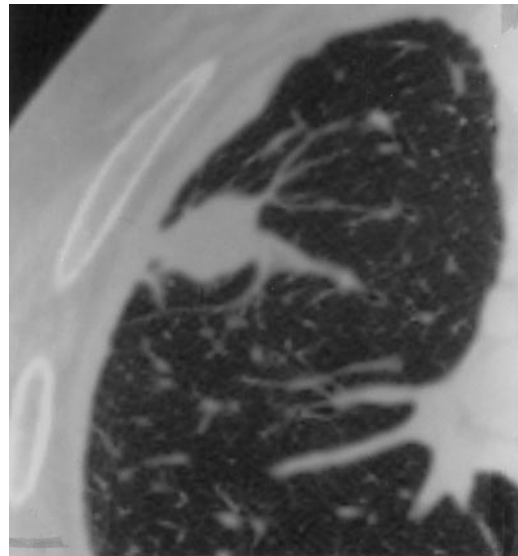
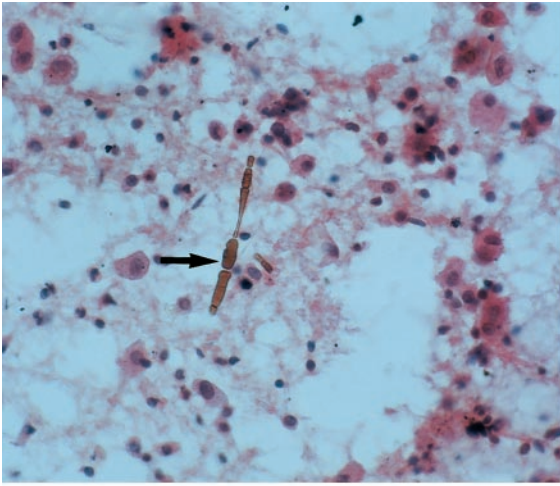


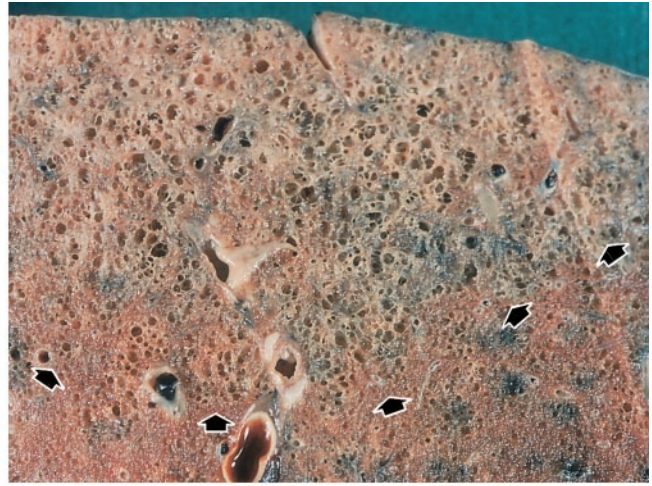
Figure 11. Axial CT scan shows an ovoid mass, pleural thickening, and linear comet tail of rounded atelectasis.

round atelectasis is also known as asbestos pseudotumor or Blesovsky syndrome.

The typical chest radiographic appearance is of a rounded peripheral “mass” with or without lung distortion (Fig 10a). Pleural thickening is usually seen. The CT features are of a round or oval mass that abuts the pleura, a “comet tail” of bronchovascular structures going into the mass, and thickening of the adjacent pleura (1,29) (Figs 10b, 11). Volume loss is often, but not invariably, apparent (30). The features can be confused with those of malignancy, with lung cancer being the main differential diagnosis.



12.



13.

Figures 12, 13. (12) Photomicrograph (original magnification, $\times 400$; hematoxylin-eosin stain) of a bronchoalveolar lavage specimen shows a classic asbestos body with a segmental dumbbell-shaped configuration (arrow). (13) Photograph shows macroscopic appearance of "honeycomb" lung with subpleural accentuation typical of asbestosis (arrows). No pleural thickening is present on this section.

Round atelectasis does show enhancement at contrast-enhanced CT (31), and it has been suggested that a uniform pattern of enhancement favors round atelectasis. However, contrast enhancement is not thought to be a reliable characteristic for differentiating benign asbestos-related disease from malignancy (1,32). Stability or shrinkage of the mass with the passage of time strongly suggests benignancy (32), but biopsy may be required.

Magnetic resonance (MR) imaging has been reported to show round atelectasis as a mass with T1 signal intensity characteristics similar to those of liver tissue and to show the vascular structures. MR imaging shows curved low-signal-intensity lines caused by thickened indentations of visceral pleura (33).

According to some authors, ultrasonography (US) may sometimes be helpful (34). The US features described are of a pleurally based mass with thickening of the adjacent pleura and extrapleural fat. An echogenic line that extends into the mass from the pleura was seen in 86% of the patients studied, a finding thought to represent the scarred invaginated visceral pleura.

Asbestosis

Asbestosis is the term given to lung fibrosis caused by asbestos dusts, which may or may not be associated with pleural fibrosis (35). There is a dose-response relationship between exposure and se-

verity of fibrosis (12,36). The lag between exposure and onset of symptoms is usually 20 years or longer (36) (sometimes more than 40 years) but can be as little as 3 years in cases with constant heavy exposure (36).

The pathogenesis of asbestosis, as with so much of asbestos-related disease, is incompletely understood. Tissue damage is caused by chemotactic factors and fibrogenic mediators released from alveolar neutrophils or macrophages after they attempt to ingest and clear the fibers. Chronic fiber deposition stimulates persistent mediator release and leads to fibrosis that spreads centrifugally from the respiratory bronchioles and alveolar ducts (36–38). Asbestos bodies are often seen within and adjacent to areas of fibrosis (Fig 12). Uncoated fibers (mainly chrysotile) may also be seen.

The changes of asbestosis are more pronounced in the lower lobes and subpleurally but often extend to involve the middle lobe and lingula. Upper lobes can be involved in advanced cases. Honeycombing, as in other fibrotic lung diseases, can occur in advanced disease (Fig 13) but is not, however, present in the majority: Aberle et al (20,26) reported its presence in 7%–17% of their cases.



a.



b.

Figure 14. (a) Posteroanterior radiograph of a patient with asbestosis shows “shaggy” mediastinal and diaphragmatic contours. (b) Localized view of the lung bases of the same patient further illustrates the diffuse interstitial opacification.

Features on chest radiographs include ground-glass opacification, small nodular opacities (36), “shaggy” cardiac silhouette, and ill-defined diaphragmatic contours (Fig 14). Honeycombing and volume loss are seen in more advanced disease. Honeycombing is not included in the quantitative part of the ILO Classification, but its presence can be recorded with the use of the additional symbols included with the classification. Pleural changes are often present in cases of asbestosis (Fig 15). It has been reported that 80% of patients with asbestosis have coexistent pleural disease at chest radiography (36), and the percentage rises to 100% with the use of high-resolution CT (20). Fibrous bands are sometimes seen to radiate inward from the pleura (36) (Fig 16). Pleural abnormalities, emphysema, or other parenchymal abnormalities can compromise the radiographic diagnosis of asbestosis (32). The sensitivity, specificity, and negative predictive value are improved by expert reading (21).

CT, especially high-resolution CT, is more sensitive than plain radiography in depicting as-



Figure 15. Posteroanterior radiograph shows diffuse fine nodular and reticular opacification with irregularity of mediastinal and diaphragmatic contours. The costophrenic angles are blunted because of pleural thickening.

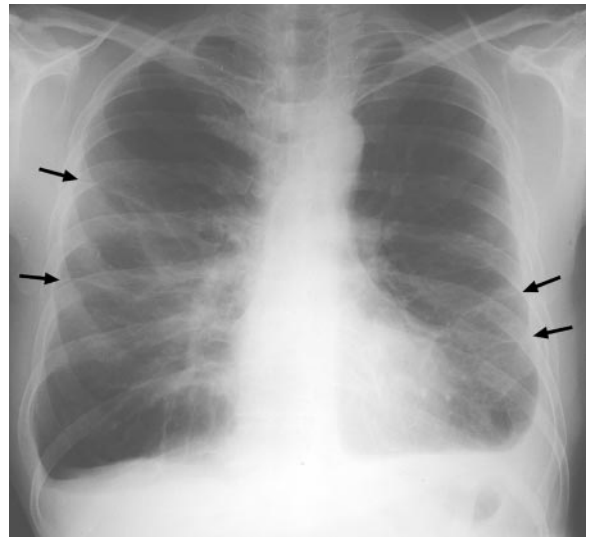
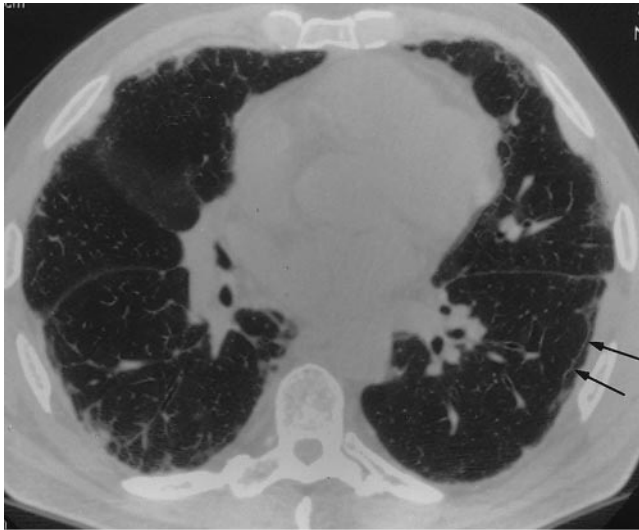
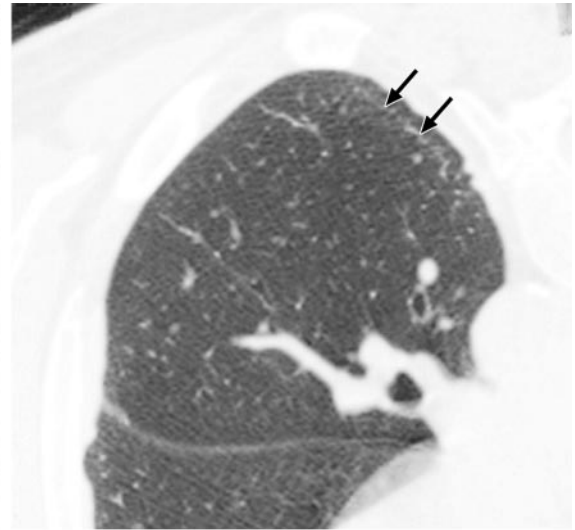


Figure 16. Posteroanterior radiograph of an asbestos-exposed person shows parenchymal bands radiating in from the pleura in both mid zones (arrows). Diffuse pleural thickening is predominantly left-sided.

bestosis. Aberle et al (26) showed that besides aiding in the confirmation of abnormal findings at chest radiography, high-resolution CT depicted changes in 80% of patients with clinical but not chest radiographic evidence of asbestosis and showed changes of asbestosis in one-third of patients with neither clinical nor chest radiographic evidence of asbestosis. Staples et al (39) showed that 57 of 169 patients with normal chest radiographic findings had high-resolution CT findings suggestive of a high probability of asbestosis. However, high-resolution CT is not infallible. Gamsu et al (40) employed a semiquantitative

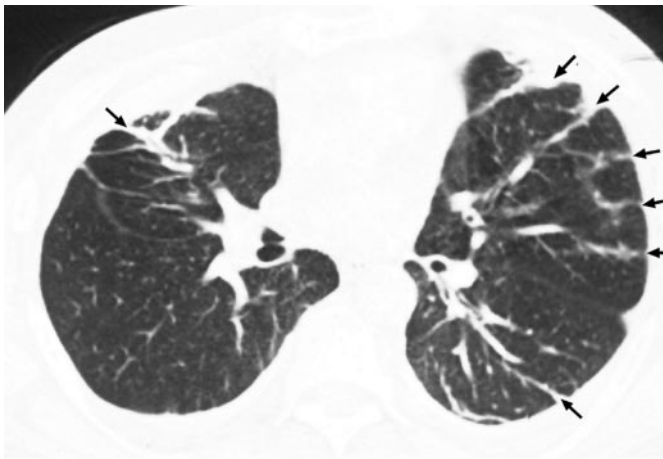


17.

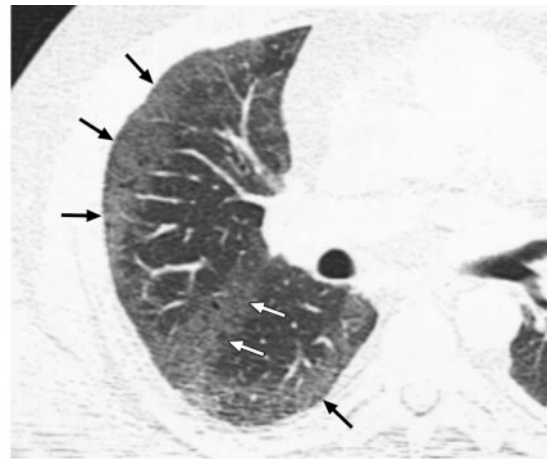


18.

Figures 17, 18. (17) Axial high-resolution CT scan shows a subpleural curvilinear opacity (arrows) thought to represent peribronchiolar fibrosis. (18) High-resolution CT scan obtained with the patient in a prone position shows early subpleural curvilinear opacity (arrows). Prone as well as supine views have been recommended (20,26) to eliminate dependent opacities.



19.



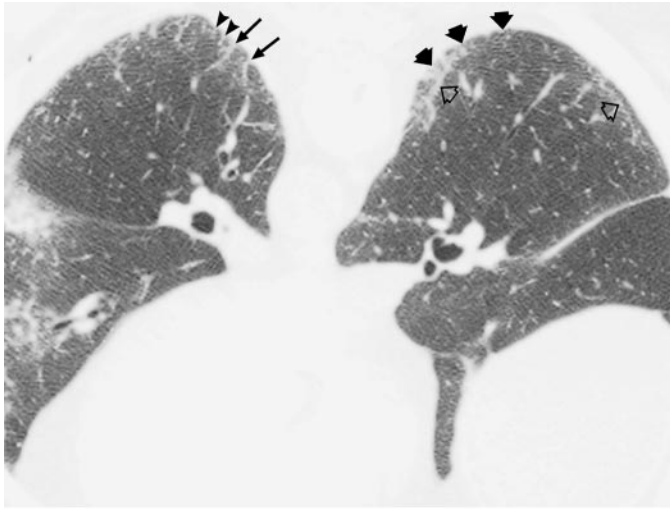
20.

Figures 19, 20. (19) High-resolution CT scan shows bilateral parenchymal bands (arrows). (20) High-resolution CT scan shows subpleural areas of ground-glass attenuation (arrows).

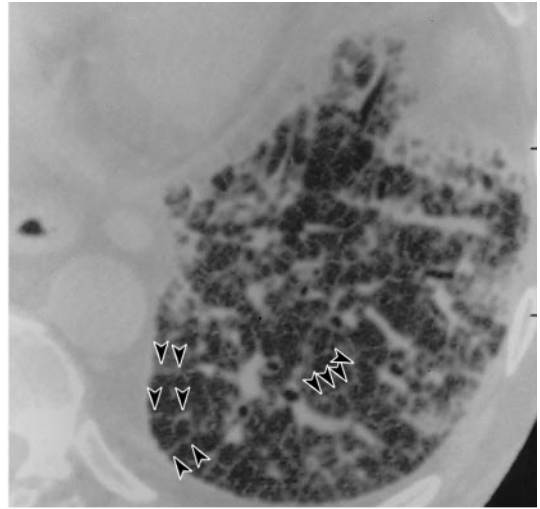
grading system in which findings of high-resolution CT were strongly positive in 64% of patients with histopathologically proved asbestosis. They also employed a cumulative method, comparing the presence or absence of five high-resolution CT features of asbestosis with the histopathologic findings. This comparison showed that any one type of abnormality was present in 88% of patients with asbestosis, two types in 78%, and three types in 56%. However, three or more abnormalities had to be present to be specific for asbestosis. Chest radiographic findings were suggestive of asbestosis in only 11 of 21 histopathologically proved cases, and 10 of 14 patients with

normal or near normal chest radiographic findings had histopathologic evidence of asbestosis.

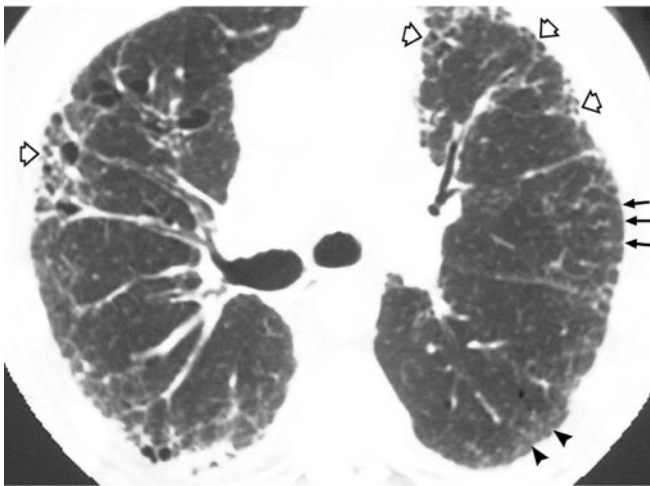
An early feature is a subpleural curvilinear opacity (Figs 17, 18). This finding represents peribronchiolar fibrosis (36,41,42). Parenchymal band-shaped opacities project in from the pleura and represent fibrosis along bronchovascular sheaths or interlobular septa (36,41,42) (Fig 19). Other features that have been reported include ground-glass opacification (due to mild alveolar wall fibrosis beyond the resolving power of CT) (Fig 20), subpleural nodular or dotlike opacities



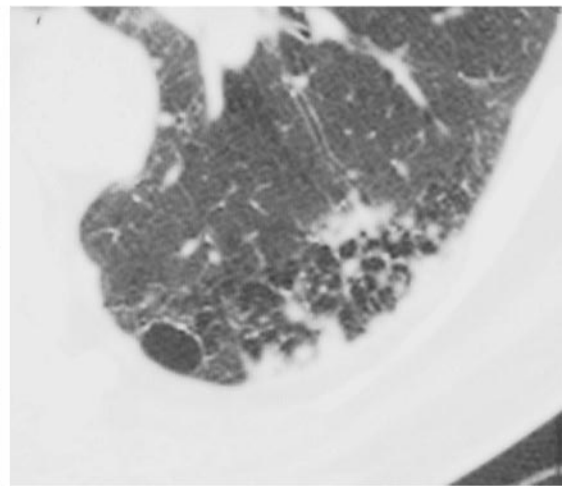
21.



22.



23.



24.

Figures 21–24. (21) Prone high-resolution CT scan shows subpleural nodular and dotlike opacities (solid wide arrows) that coalesce to form subpleural curvilinear lines (open arrows). There are also interlobular (solid thin arrows) and intralobular (arrowheads) interstitial lines. (22) High-resolution CT scan shows interlobular septal thickening (arrowheads). (23) High-resolution CT scan depicts subpleural honeycombing (open arrows), interlobular septal thickening (solid arrows), and subpleural nodular opacities (arrowheads). (24) High-resolution CT scan shows subpleural honeycombing.

(40,41), thickening of interlobular septa, and honeycombing (36) (Figs 21–24). Gamsu et al (40) found that interstitial lines (thickened interlobular septa and centrilobular core structures) were the most commonly found abnormality (84% of cases), followed by parenchymal bands

(76%) and distortion of secondary pulmonary lobules (56%). Subpleural lines and honeycombing were less frequent.

Scoring methods for disease severity have been devised with the use of high-resolution CT criteria (7,8). High-resolution CT is sometimes helpful in distinguishing asbestosis from other causes of lung fibrosis when a history of asbestos exposure is in doubt, but differentiation can be diffi-

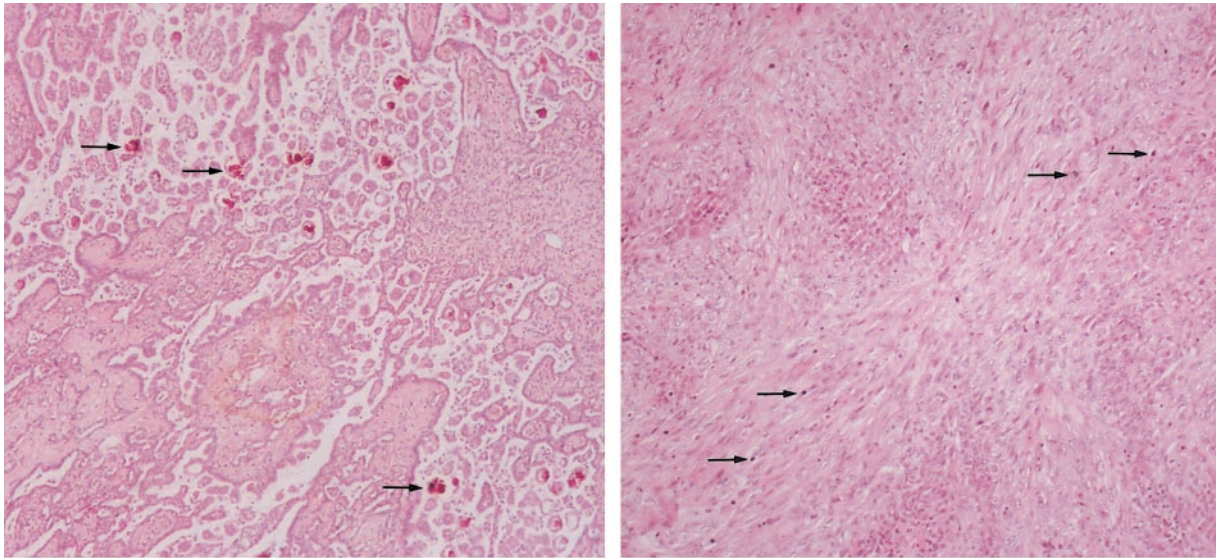


Figure 25. (a) Photomicrograph (original magnification, $\times 250$; hematoxylin-eosin stain) of a malignant mesothelioma of the epithelioid subtype shows its tubulopapillary structure and numerous scattered psammomatous bodies (arrows). (b) Photomicrograph (original magnification, $\times 400$; hematoxylin-eosin stain) shows a malignant mesothelioma of the sarcomatoid subtype: a cellular spindle cell tumor with a haphazard array of fascicles. There is marked cytonuclear pleomorphism and mitotic activity (arrows).

cult, as many of the above findings are not specific to asbestosis. The main differential diagnosis both radiologically and histopathologically is usual interstitial pneumonitis or idiopathic pulmonary fibrosis (32).

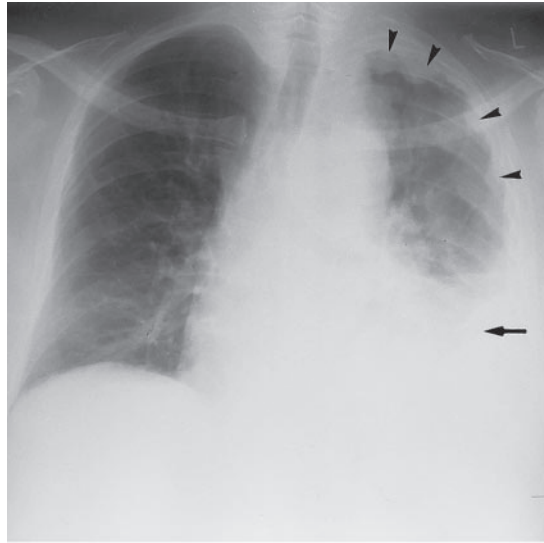
Malignant Mesothelioma

Malignant mesothelioma occurs mainly in the pleura and peritoneum but can arise in the pericardium or tunica vaginalis testis. Malignant mesothelioma is the most common primary neoplasm of the pleura (43). It has a strong association with asbestos exposure, particularly crocidolite. It has been suggested that chrysotile, unless contaminated with amphibole material, is not associated with malignant mesothelioma, but this finding is controversial (44,45). Risk ratios of the order of 1:100:500 for chrysotile, amosite, and crocidolite, respectively, have been postulated (46). Malignant mesothelioma has a latency of 35–40 years (43,47). It has a poor prognosis, with most patients dying within 1 year of diagnosis (2,48). Malignant mesothelioma can develop in patients with transient or indirect exposure to asbestos (38). Although the necessary degree of exposure is considerably less than that required

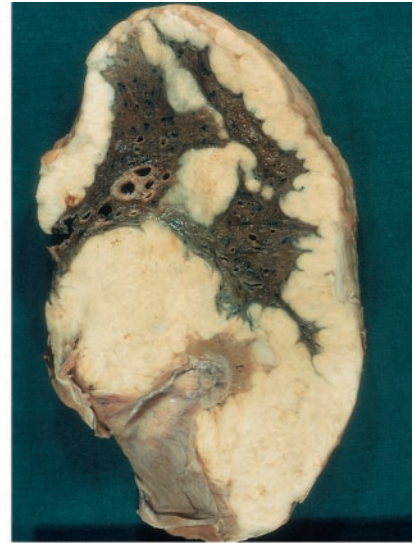
to cause asbestosis and lung cancer (4), a dose-dependent relationship has been recognized (49,50).

The tumor can arise from either pleural layer. It is often associated with an effusion. As it enlarges, it causes pleural thickening and eventual encasement of the lung with retraction of the chest wall. Direct spread into the pericardium, contralateral pleura, and peritoneum occurs. Lymph node spread occurs, as do blood-borne metastases to the lungs, liver, kidneys, and adrenal glands. The main histologic subtypes are epithelial (Fig 25a), sarcomatous (Fig 25b), and mixed. Osteosarcomatous degeneration within malignant mesothelioma has been reported (51).

Chest radiography usually shows an effusion. Pleural thickening may also be seen, and as the tumor progresses, a more lobulated outline is seen (Fig 26). The affected hemithorax becomes contracted. Tumor tissue extends into interlobar fissures (Fig 27), and chest wall involvement may be apparent. Less often, lymph node metastases, lung metastases, contralateral pleural metastases, and calcified liver metastases may be seen (48).

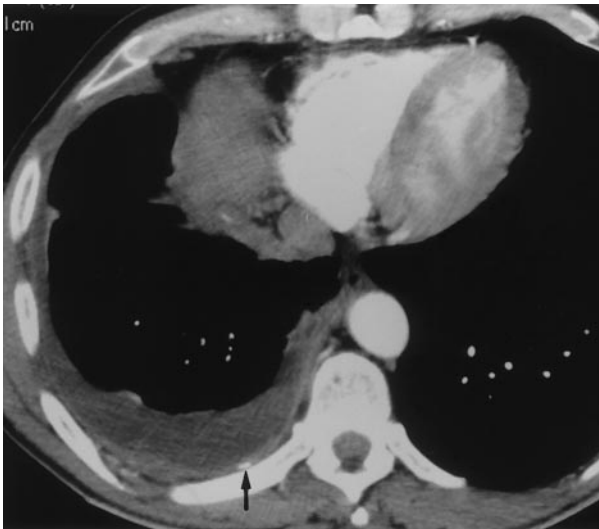


26.



27.

Figures 26, 27. (26) Posteroanterior radiograph shows left-sided lobulated thickening (arrowheads) and pleural effusion (arrow), findings characteristic of malignant mesothelioma. (27) Photograph (original magnification, approximately $\times 0.5$) of a whole lung section from a patient with malignant mesothelioma shows diffuse encasement of lung tissue by firm pale tumor tissue, with extension along the fissure.



28.

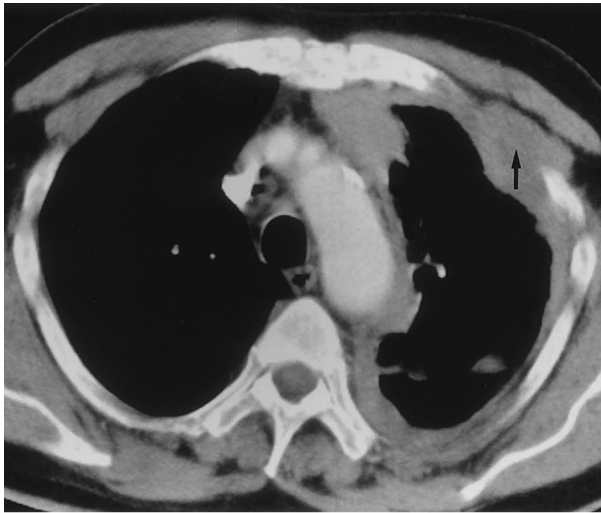


29.

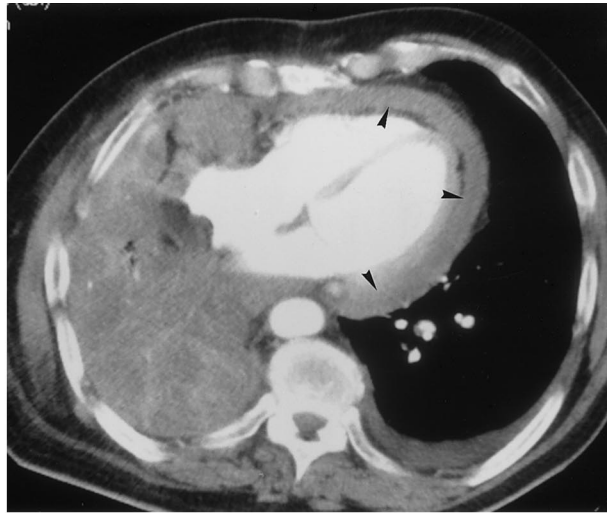
Figures 28, 29. (28) Axial CT scan of a patient with a right-sided mesothelioma shows a benign pleural plaque (arrow) engulfed by tumor tissue. (29) Axial CT scan shows a right-sided mesothelioma with extension along the major fissure (arrow) and chest wall invasion (arrowhead).

At CT, pleural thickening is the most common finding. This thickening can be lobular or smooth, and CT can help identify the disease in its early stages (52). Pleural effusions are also commonly seen. Other benign features such as pleural plaques or calcification can be seen in conjunc-

tion (Fig 28), but mesothelioma is not known to arise from plaques. CT shows contraction of the hemithorax with or without mediastinal shift; extension along fissures; invasion of the chest wall; invasion of mediastinal structures, including pericardium, great vessels, trachea, esophagus, and nodes (48); diaphragmatic invasion; and metastatic spread to nodes, the contralateral lung, or the liver (Figs 29–34).



30.

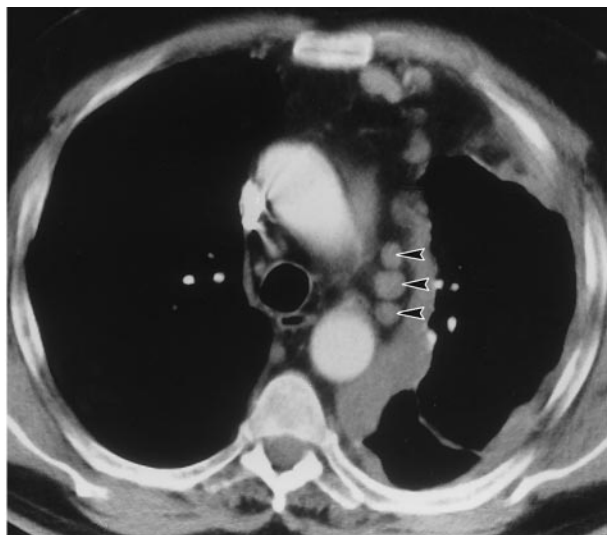


31.

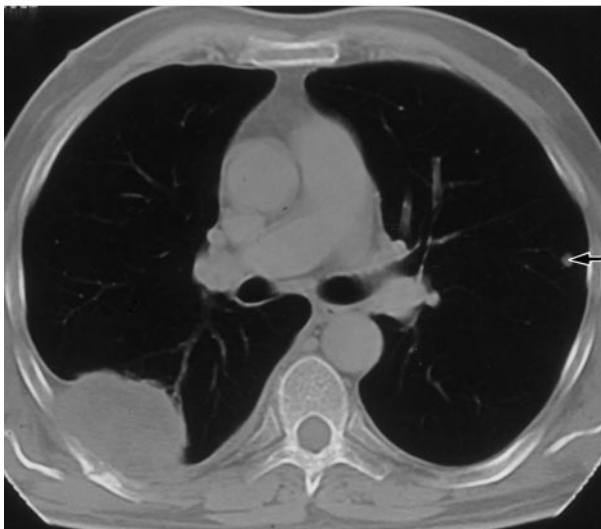
Figures 30, 31. (30) Axial CT scan of a patient with a left-sided malignant mesothelioma shows contraction of the hemithorax and chest wall invasion (arrow). (31) Axial CT scan of a patient with a right-sided mesothelioma shows invasion and encasement of the pericardium (arrowheads).



32.



33.



34.

Figures 32–34. (32) Axial CT scan of the upper abdomen shows transdiaphragmatic extension and hepatic invasion by a malignant pleural mesothelioma. (33) Axial CT scan shows a left-sided mesothelioma with mediastinal encasement and lymphadenopathy (arrowheads). (34) Axial CT scan of a patient with a right-sided mesothelioma shows a nodule in the left lung (arrow) thought to represent a metastasis. The patient did not have this finding confirmed surgically, however, owing to comorbid disease.

CT does, however, have limitations (43). CT assessment of nodes is suboptimal, with biopsy being the most accurate test (48). Assessment of transdiaphragmatic spread is limited when only axial imaging planes are used, and such spread is probably better assessed with nonaxial planes (43). It has been suggested that MR imaging is better than CT in this respect, having demonstrated 82% accuracy versus 55% with CT (48, 53). Chest wall invasion is also possibly more accurately assessed with MR imaging than with CT, MR imaging having shown 69% accuracy versus 46% for CT (48,53). These figures, however, relate to axial CT scans, and the multiplanar capabilities of multi-detector row CT may improve its accuracy in these areas. CT remains the primary staging modality, but MR imaging may provide additional information in some surgical candidates (48).

Fluorine-18 fluorodeoxyglucose positron emission tomography has been compared with CT, and uptake of F-18 fluorodeoxyglucose was found to be significantly greater in malignant mesothelioma than in benign pleural disease (sensitivity, 91%; specificity, 100%) (54). Detection of nodal disease was also improved. Spatial and anatomic detail, however, are inferior.

There is a new TNM international staging system for diffuse malignant pleural mesothelioma. This new system emphasizes criteria that help in determining local tumor extension and regional lymph node status in an attempt to identify patients with potentially curable early disease (T1a and b); those who may benefit from surgery without necessarily being cured (T2 and T3); and patients with extensive local tumor spread (T4), extensive regional node involvement, or distant metastases for whom surgery would provide no benefit (53). The system therefore stratifies patients into prognostic groups (48).

Imaging guidance can be used to obtain the necessary tissue diagnosis, but tumor spread of malignant mesothelioma along biopsy or drainage tracts is well recognized. Seeding rates of up to 22% with the use of image-guided biopsy have been reported (48). Imaging is also used to follow up patients after treatment.

The differential diagnosis of malignant mesothelioma includes benign causes of pleural thickening (such as after infection or diffuse pleural thickening) and metastatic adenocarcinoma. The lobulated outline, pleural effusion, or evidence of more advanced disease may help differentiate mesothelioma from diffuse pleural thickening. Clinical history may also point toward the diagnosis. Histologic or cytologic diagnosis is always required (48). The differentiation between



Figure 35. Photograph of a macroscopic section of an exophytic pale carcinoma in the lower lobe bronchus shows distal mucoid impaction.

mesothelioma and metastatic adenocarcinoma is difficult even with tissue biopsy. However, immunohistochemical techniques and electron microscopy have aided diagnosis (55).

Single-modality therapies (surgery, chemotherapy, or radiation therapy) have failed to significantly improve survival. Results with a multimodality approach have apparently been more favorable. Further therapies such as photodynamic therapy, targeted cytokines, and gene therapy are also being investigated (55).

Bronchogenic Carcinoma

The link between asbestos exposure and lung cancer has been suspected since the 1930s but was proved in the 1950s (56). Smoking has a more than additive effect. Amphiboles are more potent than chrysotile in inducing lung cancer (between 10 and 50 times greater potency has been quoted [46]). The latent period is variable. Some cases occur less than 10 years after exposure, but the risk is increased until at least 30 years later (57). One report cited a lag of 50 years (58).

The exact mechanism of carcinogenesis is unclear. Asbestos-related cancers can occur anywhere in the lungs (Figs 35, 36). The evidence regarding a link between asbestos and a particular histologic type or lobar distribution of lung cancer is somewhat contradictory (59).

The investigation and staging of asbestos-related lung cancers are the same as for non-asbes-



Figure 36. Axial CT scan shows a large left lower lobe carcinoma in a patient with asbestos-related plaques (arrows).

tos-related cancers. The prognosis is similar to that for non-asbestos-related lung cancers, but the restrictive effect of coexistent asbestosis or diffuse pleural thickening could compromise patients' respiratory function and fitness for attempted resection.

Other Pathologic Conditions

Other tumors to which asbestos has been linked include peritoneal mesothelioma and carcinoma of the larynx and kidney. Asbestos has also been suggested as a contributor to nodular pulmonary amyloidosis (60).

Conclusion

It is important to be aware of the clinical, radiologic, and pathologic characteristics of asbestos-related diseases, as they will persist for some time, especially asbestosis and malignant mesothelioma, which appear to have the longest latency. For these diseases, it is certain that it will be some time before the dust has settled.

References

1. Peacock C, Copley SJ, Hansell DM. Asbestos-related benign pleural disease. *Clin Radiol* 2000; 55:422–432.
2. Peto J, Hodgson JT, Matthews FE, Jones JR. Continuing increase in mesothelioma mortality in Britain. *Lancet* 1995; 345:535–539.
3. Consensus Report. International expert meeting on new advances in the radiology and screening of asbestos-related diseases. *Scand J Work Environ Health* 2000; 26:449–454.
4. Report by the Industrial Injuries Advisory Council in accordance with Section 171 of the Social Security Administration Act 1992: asbestos related diseases. London, United Kingdom: Her Majesty's Stationery Office, 1996.
5. International Labour Office: Guidelines for the use of ILO international classification of radiographs of pneumoconiosis, 1980 ed. Geneva, Switzerland: International Labour Office, 1980.
6. Shipley RT. The 1980 ILO Classification of the radiographs of the pneumoconioses. *Radiol Clin North Am* 1992; 30:1135–1145.
7. Huuskonen O, Kivisaari L, Zitting A, et al. High-resolution computed tomography classification of lung fibrosis for patients with asbestos-related disease. *Scand J Work Environ Health* 2001; 27:106–112.
8. Suganuma N, Kusaka Y, Hosoda Y, et al. The Japanese classification of computed tomography for pneumoconiosis with standard films: comparison with the ILO International Classification of radiographs for pneumoconiosis. *J Occup Health* 2001; 43:24–31.
9. Aberle DR, Balmes JR. Computed tomography of asbestos-related pulmonary parenchymal and pleural diseases. *Clin Chest Med* 1991; 12:115–131.
10. Eisenstadt HB. Asbestos pleurisy. *Dis Chest* 1964; 46:78–81.
11. Epler GR, McLoud TC, Gaensler EA. Prevalence and incidence of benign asbestos pleural effusion in a working population. *JAMA* 1982; 247:617–622.
12. Kim KI, Kim CW, Lee MK, et al. Imaging of occupational lung disease. *RadioGraphics* 2001; 21:1371–1391.
13. Hillerdal G, Ozesmi M. Benign asbestos pleural effusion: 73 exudates in 60 patients. *Eur J Resp Dis* 1987; 71:113–121.
14. Fletcher DE, Edge JR. The radiological changes in pulmonary and pleural asbestosis. *Clin Radiol* 1970; 21:355–365.
15. Hu H, Beckett L, Kelsey K, Christiani D. The left-sided predominance of asbestos-related pleural disease. *Am Rev Respir Dis* 1993; 148:981–984.
16. Gallego JC. Absence of left-sided predominance in asbestos-related pleural plaques: a CT study. *Chest* 1998; 113:1034–1036.
17. Sebastien P, Janson X, Gaudichet A, Hirsch A, Bignon J. Asbestos retention in human respiratory tissues: comparative measurements in lung parenchyma and in parietal pleura. *IARC Sci Publica* 1980; 237–246.
18. Hillerdal G. The pathogenesis of pleural plaques and pulmonary asbestosis: possibilities and impossibilities. *Eur J Resp Dis* 1980; 61:129–138.
19. Al Jarad N, Poulakis N, Pearson MC, Rubens MB, Rudd RM. Assessment of asbestos-induced pleural disease by computed tomography: correlation with chest radiograph and lung function. *Respir Med* 1991; 85:203–208.
20. Aberle DR, Gamsu G, Ray CS, Feuerstein IM. Asbestos-related pleural and parenchymal fibrosis: detection with high-resolution CT. *Radiology* 1988; 166:729–734.
21. Friedman AC, Fiel SB, Fisher MS, Radecki PD, Lev-Toaff AS, Caroline DF. Asbestos-related pleural disease and asbestosis: a comparison of CT and chest radiography. *AJR Am J Roentgenol* 1988; 150:269–275.
22. Stephens M, Gibbs AR, Pooley FD, Wagner JC. Asbestos induced diffuse pleural fibrosis: pathology and mineralogy. *Thorax* 1987; 42:583–588.

23. Frank W, Loddenkemper R. Fiber-associated pleural disease. *Semin Respir Crit Care Med* 1995; 16:315–323.
24. McLoud TC, Woods BO, Carrington CB, Epler JR, Gaensler EA. Diffuse pleural thickening in the asbestos-exposed population. *AJR Am J Roentgenol* 1985; 144:9–18.
25. Lynch DA, Gamsu G, Aberle DR. Conventional and high-resolution tomography in the diagnosis of asbestos-related diseases. *RadioGraphics* 1989; 9:523–551.
26. Aberle DR, Gamsu G, Ray CS. High-resolution CT of benign asbestos-related diseases: clinical and radiographic correlation. *AJR Am J Roentgenol* 1988; 151:883–891.
27. Copley SJ, Wells AU, Rubens MB, et al. Functional consequences of pleural disease evaluated with chest radiography and CT. *Radiology* 2001; 220:237–243.
28. Blesovsky A. The folded lung. *Br J Dis Chest* 1966; 60:19–22.
29. McHugh K, Blaquiére RM. CT features of rounded atelectasis. *AJR Am J Roentgenol* 1989; 257–260.
30. Lynch DA, Gamsu G, Ray CS, Aberle DR. Asbestos-related focal lung masses: manifestations on conventional and high-resolution CT scans. *Radiology* 1988; 169:603–607.
31. Taylor PM. Dynamic contrast enhancement of asbestos-related pulmonary pseudotumours. *Br J Radiol* 1988; 61:1070–1072.
32. Staples CA. Computed tomography in the evaluation of benign asbestos-related disorders. *Radiol Clin North Am* 1992; 30:1191–1207.
33. Verschakelen JA, Demaerel P, Coolen J, Demedts M, Marchal G, Baert AL. Rounded atelectasis of the lung: MR appearance. *AJR Am J Roentgenol* 1989; 152:965–966.
34. Marchbank ND, Wilson AG, Joseph AE. Ultrasound features of folded lung. *Clin Radiol* 1996; 51:433–437.
35. Acheson ED, Gardner MJ. The ill-effects of asbestos upon health. Asbestos: final report of the advisory committee, vol 2. London, United Kingdom: Her Majesty's Stationery Office, 1979.
36. Dee P. Inhalational lung diseases. In: Armstrong P, Wilson AG, Dee P, Hansell DM, eds. *Imaging of diseases of the chest*. 3rd ed. London, United Kingdom: Mosby, Harcourt, 2000; 485.
37. Robbins SL, Cotran RS, Kumar V, eds. *Robbins pathologic basis of disease*. 6th ed. Philadelphia, Pa: Saunders, 1999; 732–734.
38. Craighead JE, Mossman BT. The pathogenesis of asbestos-related diseases. *N Engl J Med* 1982; 306:1446–1455.
39. Staples CA, Gamsu G, Ray CS, Webb WR. High resolution computed tomography and lung function in asbestos-exposed workers with normal chest radiographs. *Am Rev Resp Dis* 1989; 139: 1502–1508.
40. Gamsu G, Salmon CJ, Warnock, Blanc PD. CT quantification of interstitial fibrosis in patients with asbestosis: a comparison of two methods. *AJR Am J Roentgenol* 1995; 164:63–68.
41. Akira M, Yokoyama K, Yamamoto S, et al. Early asbestosis: evaluation with high-resolution CT. *Radiology* 1991; 178:409–416.
42. Akira M, Yamamoto S, Yokoyama K, et al. Asbestosis: high-resolution CT–pathologic correlation. *Radiology* 1990; 176:389–394.
43. Ng CS, Munden RF, Libshitz HI. Malignant pleural mesothelioma: the spectrum of manifestations on CT in 70 cases. *Clin Radiol* 1999; 54: 415–421.
44. Yano E, Wang ZM, Wang XR, Wang MZ, Lan YJ. Cancer mortality among workers exposed to amphibole-free chrysotile asbestos. *Am J Epidemiol* 2001; 154:538–543.
45. Suzuki Y, Yuen SR. Asbestos tissue burden study on human malignant mesothelioma. *Ind Health* 2001; 39:150–160.
46. Hodgson JT, Darnton A. The quantitative risks of mesothelioma and lung cancer in relation to asbestos exposure. *Ann Occup Hyg* 2000; 44:565–601.
47. Miller BH, Rosado-de-Christenson ML, Mason AC, et al. Malignant pleural mesothelioma: radiologic-pathologic correlation. *RadioGraphics* 1996; 16:613–644.
48. Marom EM, Erasmus JJ, Pass HI, Patz EF Jr. The role of imaging in malignant pleural mesothelioma. *Semin Oncol* 2002; 29:26–35.
49. Al Jarad N. Asbestos-related disease. *J R Coll Physicians Lond* 1999; 33:532–536.
50. Hillerdal G. Malignant mesothelioma 1982: review of 4710 published cases. *Br J Dis Chest* 1983; 77:321–343.
51. Raizon A, Schwartz A, Hix W, Rockoff SD. Calcification as a sign of sarcomatous degeneration of malignant pleural mesotheliomas: a new CT finding. *J Comput Assist Tomogr* 1996; 20:42–44.
52. Bandoh S, Fujita J, Fukunaga Y, et al. Nodular thickening of interlobar fissures: an early manifestation of malignant mesothelioma: a case report. *Jpn J Clin Oncol* 2001; 31:82–85.
53. Heelan RT, Rusch VW, Begg CB, Panicek DM, Caravelli JF, Eisen C. Staging of malignant pleural mesothelioma: comparison of CT and MR imaging. *AJR Am J Roentgenol* 1999; 172:1039–1047.
54. Benard F, Sterman D, Smith RJ, et al. Metabolic imaging of malignant pleural mesothelioma with fluorodeoxyglucose positron emission tomography. *Chest* 1998; 114:713–722.
55. Jaklitsch MT, Grondin SC, Sugarbaker DJ. Treatment of malignant mesothelioma. *World J Surg* 2001; 25:210–217.
56. Doll R. Mortality from lung cancer in asbestos workers. *Br J Ind Med* 1955; 12:81.
57. Doll R, Peto J. Asbestos: effects on health of exposure to asbestos. London, United Kingdom: Health and Safety Commission, Her Majesty's Stationery Office, 1985.
58. Hiraoka T, Watanabe A, Usuma Y, et al. An operated case of lung cancer with pleural plaques: its asbestos bodies, fiber analysis and asbestos exposure. *Ind Health* 2001; 39:194–197.
59. Lee BW, Wain JC, Kelsey KT, Wiencke JK, Christiani DC. Association of cigarette smoking and asbestos exposure with location and histology of lung cancer. *Am J Respir Crit Care Med* 1998; 157:748–755.
60. Hiroshima K, Ohwada H, Ishibashi M, et al. Nodular pulmonary amyloidosis associated with asbestos exposure. *Pathol Int* 1996; 46:66–70.